January 24, 2005

Water Cherenkov Test Stand Calculations

Milind Diwan

Brookhaven National Laboratory
Box 5000, Upton, NY 11973-5000

1 Introduction

Our goal is to evaluate large area ($> 1\ cm^2$) avalanche photodiodes for use as water Cherenkov detectors. It is clear that the main problem is the ability to detector single photo electrons. At the moment it is unclear how we will achieve this, nevertheless it is valuable to understand the yield of detected Cherenkov photons on such a detector. By comparing with well characterized photo-multiplier tubes we should be able to measure the efficiency of APDs for detecting this light under water. Furthermore, during the course of this work we will learn how to operate this device immersed in water. We need to design a test apparatus to trigger on the vertical cosmic rays and collect the light on a detector.

2 Requirements

Some requirements and conditions for the cosmic ray water Cherenkov test stand are listed here:

- Event Rate: For good statistics we want at least a few events per hour. We assume that we will define cosmics by using two square counters, each with dimensions of $a \times a$ separated vertically by distance d. The rate of cosmic rays at the surface about the vertical is given by $I_\nu \approx 110/m^2/sec/sr$. Out of this $80/m^2/sec/sr$ is the "hard" muon type component and rest is "soft" electron like component[1]. The rate of events in the test stand will be $R = I_\nu \times a^4/d^2$. We will assume $d = 100\ cm$. Then for the hard component, $R = 0.23,\ 0.73,\ 3.7,\ 28.8$ per hour for $a = 3\ cm, 4\ cm, 6\ cm, 10\ cm$, respectively. Obviously the optics for collecting the light will be easier for small values of a, but we also need sufficient number of events. For the rest of this calculation we will assume $a = 6\ cm$.

  The mean muon energy at ground level is $\sim 4\ GeV$. The muon spectrum at sea level is flat up to $\sim 1\ GeV$ and then steepens to $E^{-2.7}$ in the 10-100 GeV range. We will assume for our purposes a flat spectrum from 0.5 to 10 GeV. Muons at 0.5 GeV/c have velocity of $0.97742 \times c$. They will have a Cherenkov cone with an angle smaller by about 1.5^o compared to highly relativistic muons. This will cause some aberration of the focus. We will take this into account in our calculation.

- Photo-sensor size: The size of the photo-sensors of interest will be approximately 1 cm^2. The RMD APD sensors are square in shape. Some API APDs, and most

photo-multiplier tubes have a circular shape. We will make sure sensors up to 2 *inch* in diameter can be accommodated. The recently developed immersible RMD APD sensor is shown in Figure 1.

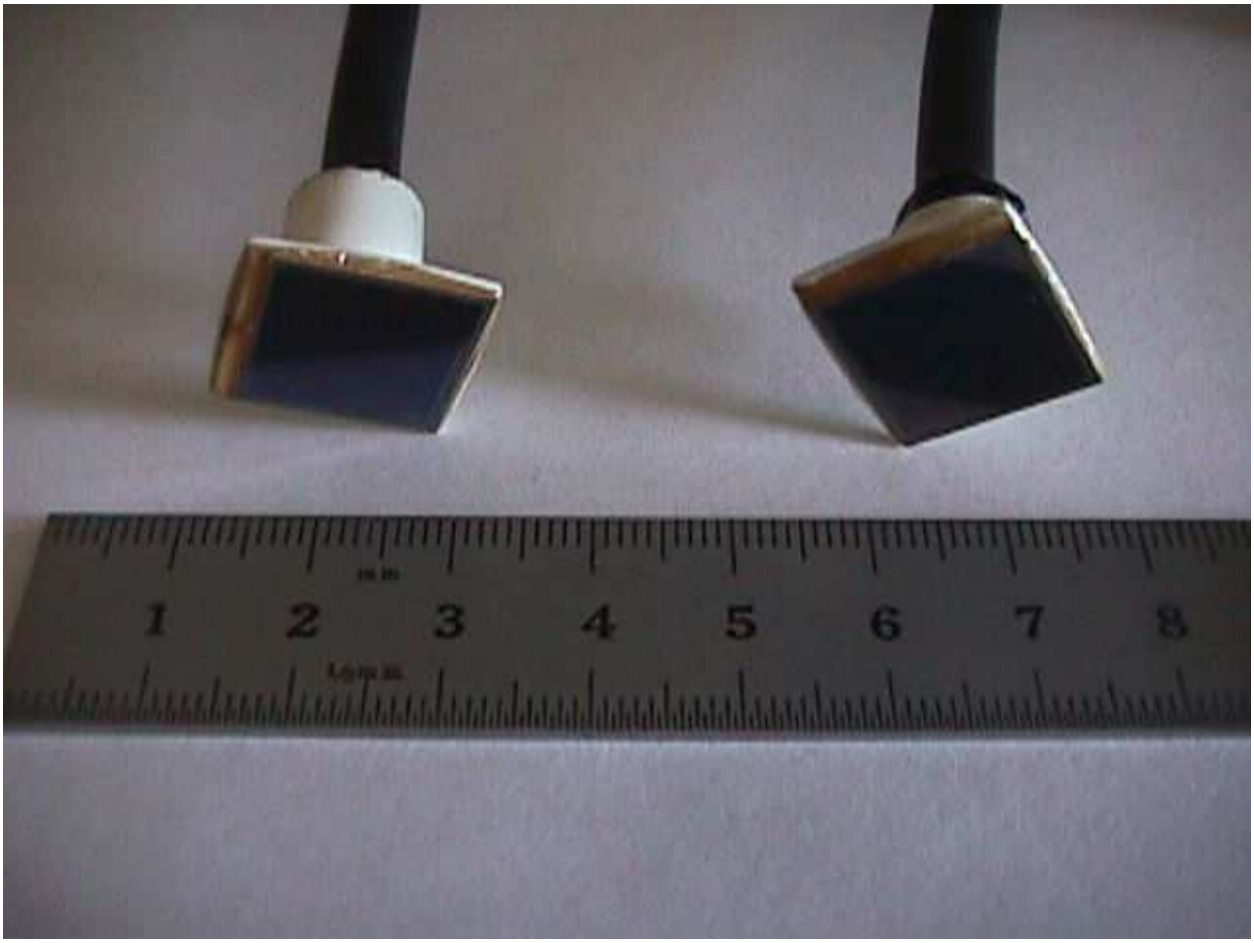

Figure 1: RMD avalanche photodiode that can be placed under water. The high voltage cable is coming from the back of the sensor and is sealed from water. (photograph from Richard Farrell.)

- Strength of signal: To get a good signal to noise ratio for APDs we need at least 50 photons striking the photo-sensor. We will have to make sure the light collection optics will provide this kind of intensity for most of the muons defined by the geometry described above ($a = 6\ cm$).
- Water condition: We will need to keep the water clean. Since the volume is small ($\sim$100-200 liters), we can always start with distilled water. We need to be careful

T/ ^oC	226.50 nm	361.05 nm	404.41 nm	589.00 nm	632.80 nm	1013.98 nm
0	1.39450	1.34896	1.34415	1.33432	1.33306	1.32612
20	1.39336	1.34795	1.34315	1.33346	1.33211	1.32524

Table 1: Dependence of the index of refraction on the temperature and wavelength in water.

about the quality of the inner surfaces, so that we don't get too much corrosion. We should also have a provision for filtering the water continuously.

- Water temperature: The APDs will have better signal to noise ratio at lower temperatures. The easiest way to cool them might be to keep the water at a low fixed temperature. The temperature needs to be maintained constant within about 0.1^oC.

- Wavelengths: The wavelengths of interest are from 300 nm to about 600 nm. Water absorbs strongly above and below this range. Since Cherenkov light intensity falls as $1/\lambda^2$, the lower wavelengths are more important. We will have to make sure that the mirror and any windows or coatings on the photo-sensor do not affect wavelengths down to 300 nm. The peak of the spectrum from water will be about $\sim 370nm$ (Fig. 2). For our simulations we will assume a flat distribution between 350 nm and 450 nm. Table 1 shows the temperature and wavelength dependence of the index of refraction [2]. In Figures 3 and 4 we display the attenuation length in water as a function of wavelength [3, 4, 5, 6, 7]. Figure 4 shows the attenuation that was achieved in the Super-Kamikande detector.

3 Optimization of the design

The number of photons produced per unit path length (x) of a particle of charge ze per unit wavelength (λ) is given by:

$$\frac{d^2N}{dxd\lambda} = \frac{2\pi\alpha z^2}{\lambda^2}(1 - \frac{1}{\beta^2 n_r^2(\lambda)}). \quad (1)$$

Here β is the velocity (in units of the speed of light c) of the charged particle and n_r is the index of refraction. For water, the index of refraction is given in Table 1. Assuming no absorption and unit detection efficiency, the yield from water in the 300 to 600 nm range should be $\sim$ 328 photons per cm of track. If water can be kept pure, and short

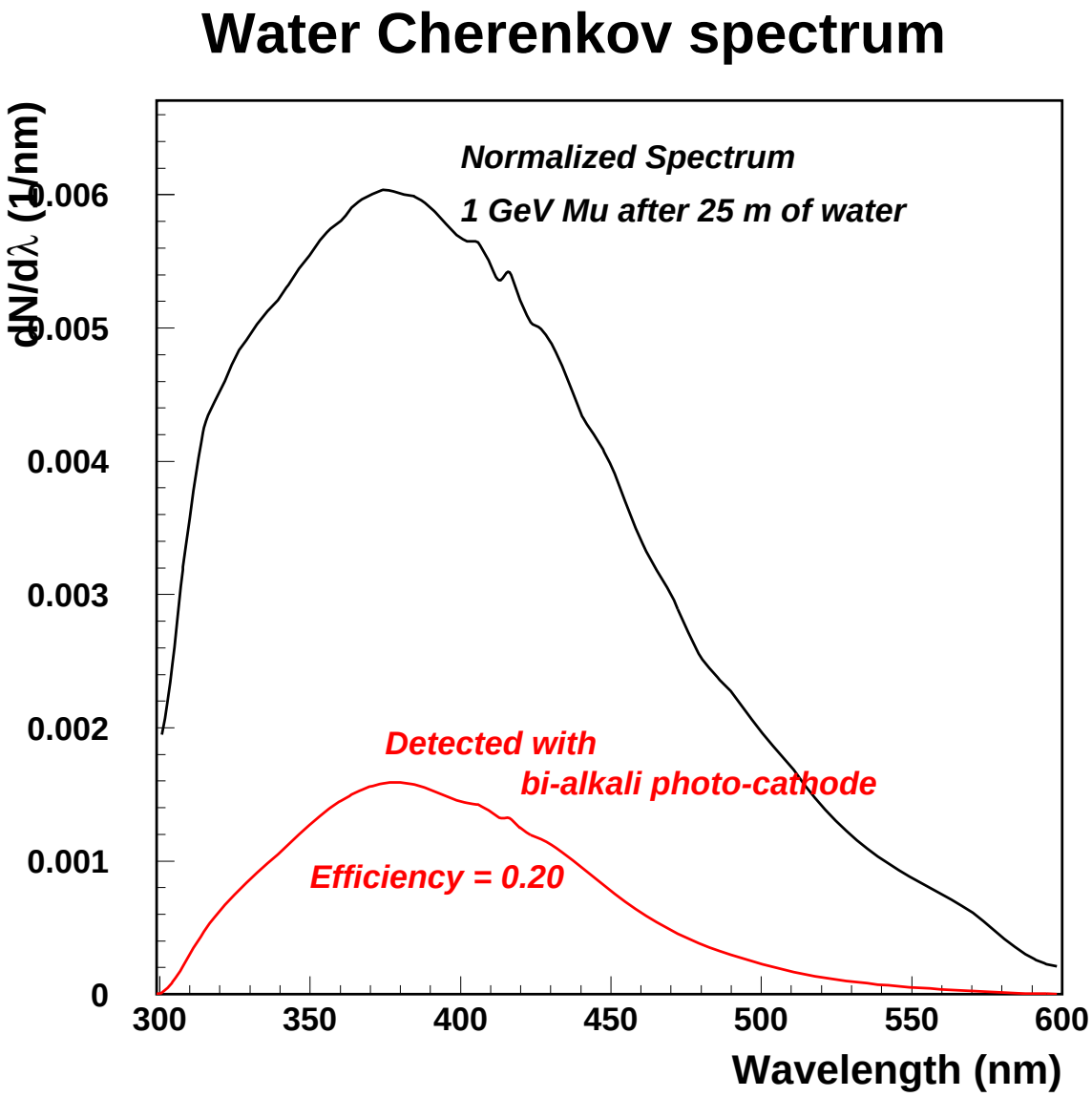

Figure 2: Spectrum of light from a 1 GeV muon in a water Cherenkov tank after 25 meters of propagation. For the short tank we are considering, the spectrum will be higher at both low and high wavelengths.

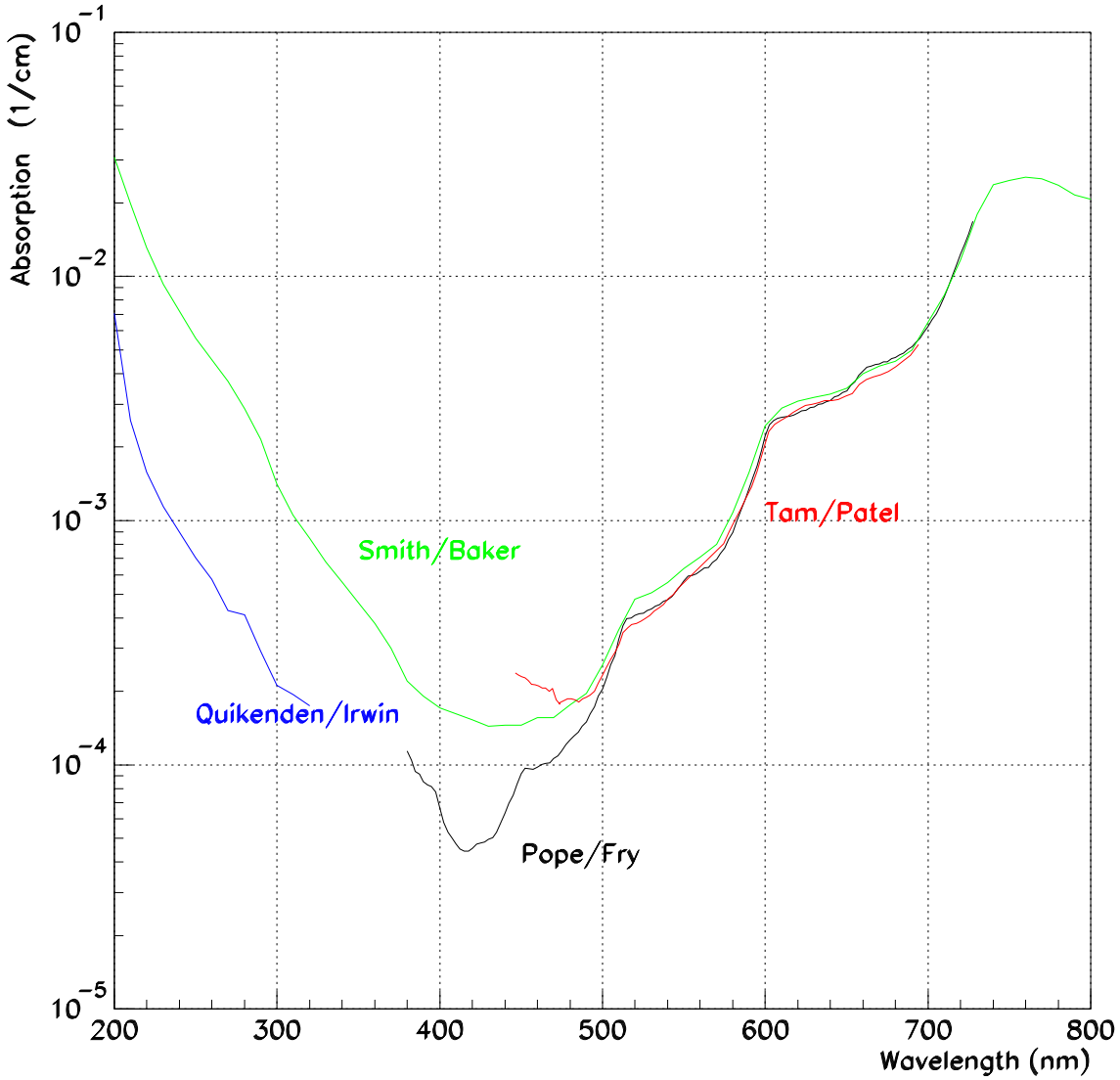

Figure 3: Attenuation length in water as a function of wavelength from various published data. The Smith and Baker numbers are for natural clear bodies of water. The other numbers are more relevant for laboratory grade pure water.

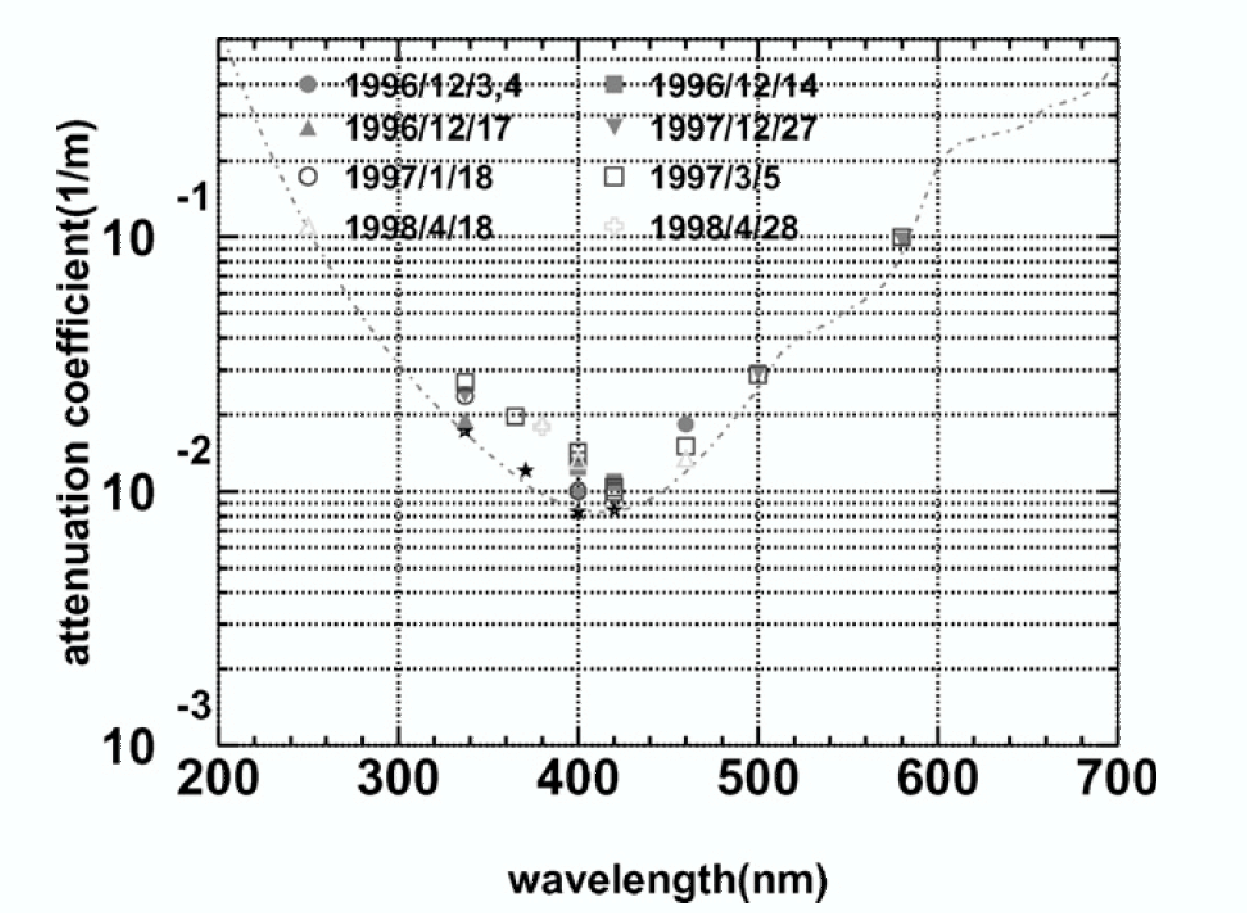

Figure 4: Attenuation length as measured in the Super-Kamiokande detector. The dashed line is the model of attenuation used by the experiment, it includes Rayleigh and Mie scattering as well as absorption. The data points are measurements described in [7].

wavelengths ($< 350\ nm$) can be detected the absorption should be about 3% integrated over the wavelength spectrum (Figure 5). For the calculation below we will use a yield of ~ 200 per cm assuming that we can only access wavelengths between 350 and 550 nm. n_r is dependent on the wavelength of light that is emitted. θ_c is the half angle of the Cherenkov cone of light emitted from the charged particle. It is given by:

$$\theta_c = \arccos(\frac{1}{\beta n_r})$$

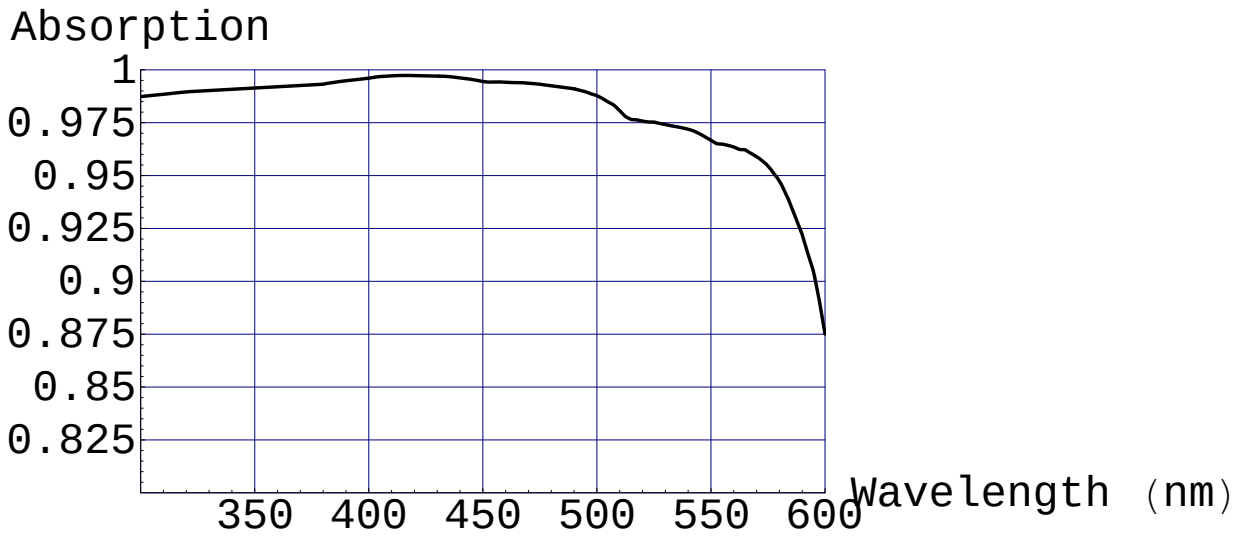

Figure 5: Calculated absorption as a function of wavelength for 60 cm of water.

Figure 6 shows the schematic of the proposed optics. The equation that describes the shape of the mirror is given by

$$\frac{dy}{dx} = \tan\left(\frac{\theta_c}{2} + \frac{1}{2}\arctan\frac{x}{(L_f - y)}\right) \tag{2}$$

This equation is good for all values of L_f, where L_f is the distance from the bottom of the mirror to the focal point. We assume that the mirror diameter is d and the shape of the mirror is given by a function $C_m(x)$ with $C_m(0) = 0$. For a muon on the axis of the mirror,

the mirror will collect light from a track length given by $T = d/\tan\theta_c + C_m(d)$. So as not to obstruct the light collection area the focal point (where the detector will be located) needs to be located at a distance $L_f > T$. When d approaches L_f the shape of the mirror will become steep at the edges. The reflectivity as well as practical considerations, therefore, limit L_f to be longer than the diameter of the mirror. If L_f is made too large, however, the light collection for off-axis muons will become worse. As noted in the previous section, we need to get good signals from muons going through two of scintillation counters, each $6cm \times 6cm$ separated by 1 m.

With above considerations (as well as ease of fabrication) in mind I have selected $d = 30cm$. In the following section I will compute the light yield into a detector of diameter 1 cm located at the focal point for $L_f = 25,\ 30,\ 35\ cm$.

4 Calculations

Equation 2 can be solved numerically for the dimensionless function, S, so that $C_m(x) = L_f \times S(x/L_f)$.

Using the value of $n_r = 1.34315$ and $\beta = 1$ we obtain $\theta_c = 41.8822^o$; this sets the shape of the mirror. For this and other values of n_r the shape of the mirror is shown in figure 7. For our design we have used $n_r = 1.34315$.

The numerical solution shown in Figure 7 can be approximated by a polynomial. We calculated the approximation by making a fit to 20 points along the curve for $n_r = 1.34315$ (see Table 2) . The approximation is given by

$$\begin{aligned} \frac{C_m(x/L_f)}{L_f} &= 0.379642(x/L_f) + 0.336509(x/L_f)^2 \\ &\quad -0.166823(x/L_f)^3 + 0.740076(x/L_f)^4 \\ &\quad -0.773981(x/L_f)^5 + 0.38747(x/L_f)^6 \end{aligned} \tag{3}$$

The difference between the approximation and the numerical solution is shown in Figure **??**. For $L_f = 25cm$ the maximum error can be read from the figure to be $\sim 15\mu m$. Any error from mirror manufacturing should be kept below this value.

In Figure 9 we show the light distribution from an ideal muon on the axis of the mirror. The muon is assumed to be on the axis of the mirror. The light is generated assuming a flat distribution for muon momentum between 0.5 and 10 GeV. We also assume a flat distribution

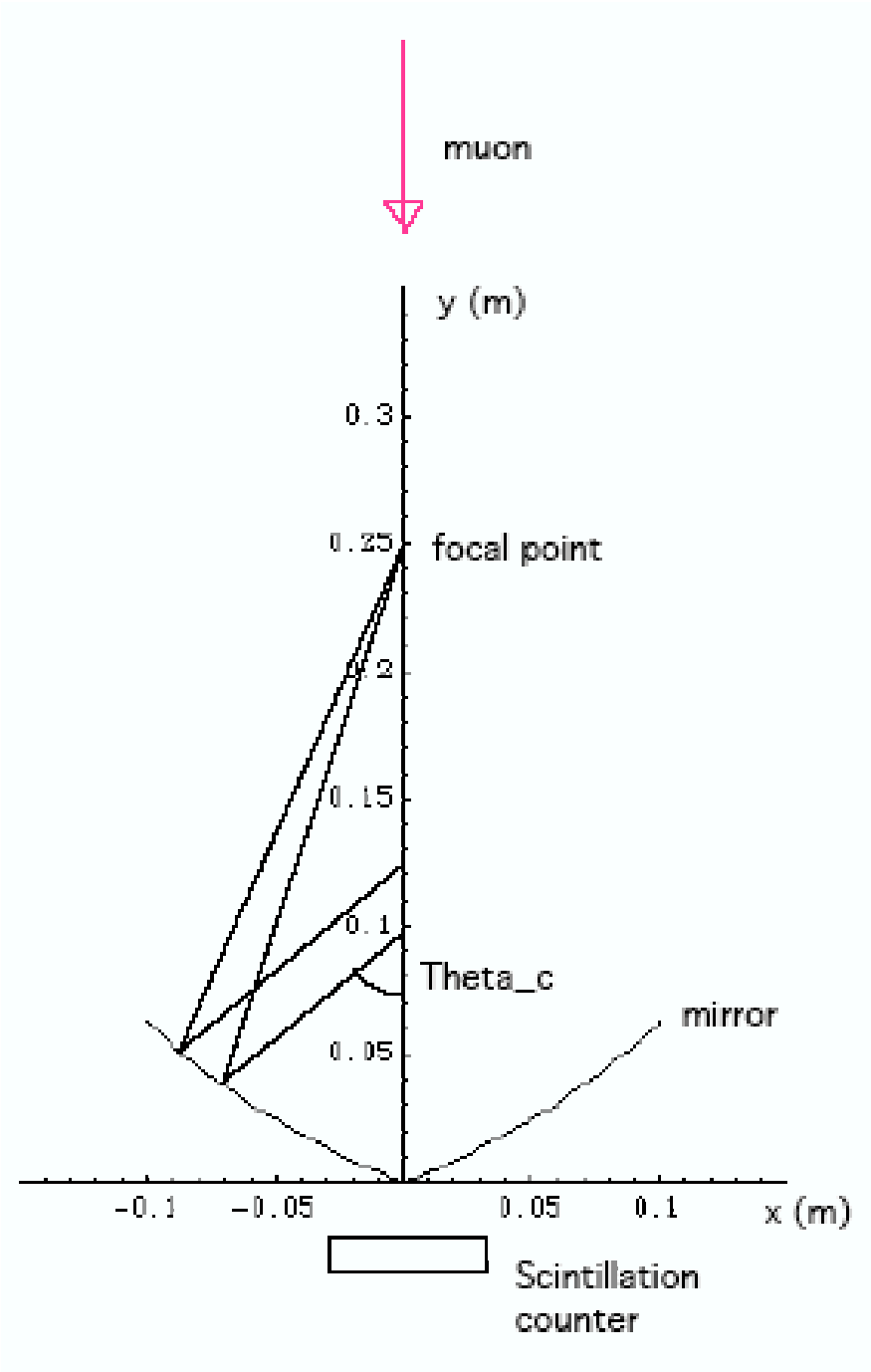

Figure 6: Schematic of the optics to collect Cherenkov light from downward going cosmic ray muons.

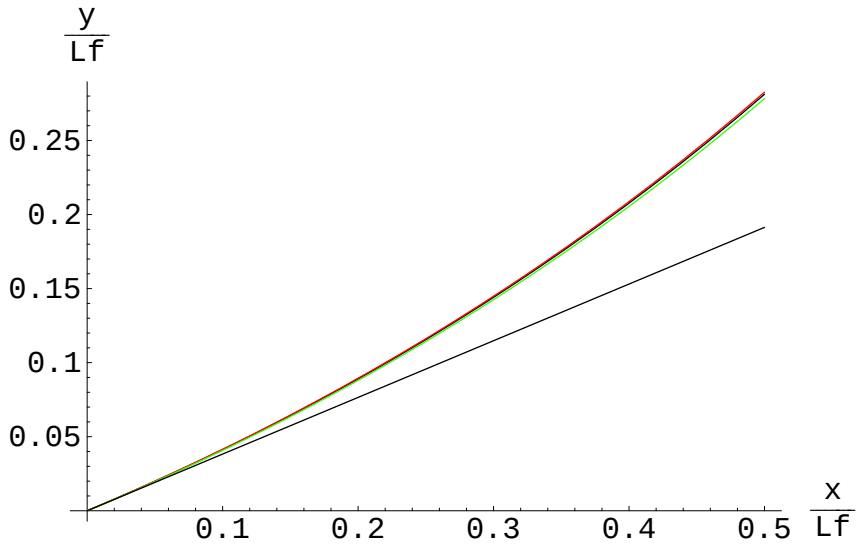

Figure 7: Shape of the mirror for three values of n_r, 1.34795 (red), 1.34315(black), 1.33336 (green). The shape of a cone with half angle of $\theta_c = 41.8822^o$ is also shown.

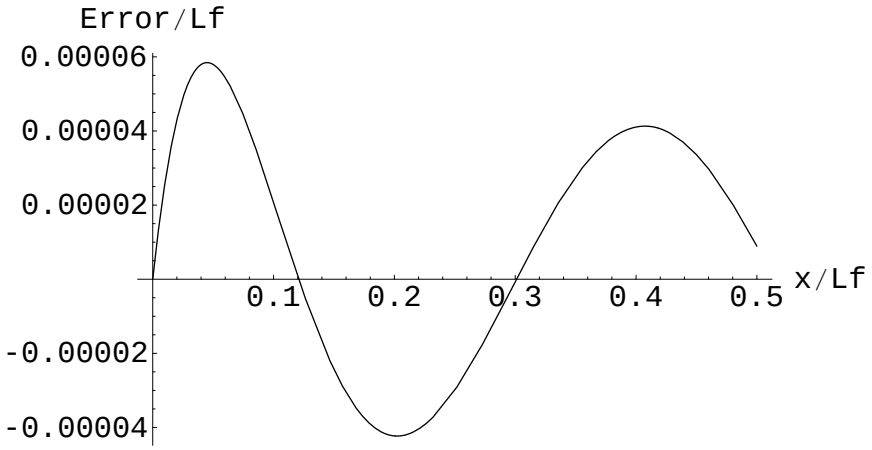

Figure 8: Difference between the shape of the mirror from the numerical calculation and the approximation in Equation 3. ($n_r = 1.34315$)

x/L_f	$S(x/L_f)$
0	0
0.025	0.009748
0.05	0.019865
0.075	0.030362
0.1	0.041250
0.125	0.052542
0.15	0.064251
0.175	0.076390
0.2	0.088973
0.225	0.102016
0.25	0.115535
0.275	0.129547
0.3	0.144070
0.325	0.159122
0.35	0.174725
0.375	0.190900
0.4	0.207670
0.425	0.225060
0.45	0.243097
0.475	0.261809
0.5	0.281226

Table 2: Numerical solution to equation 2 at 20 points.

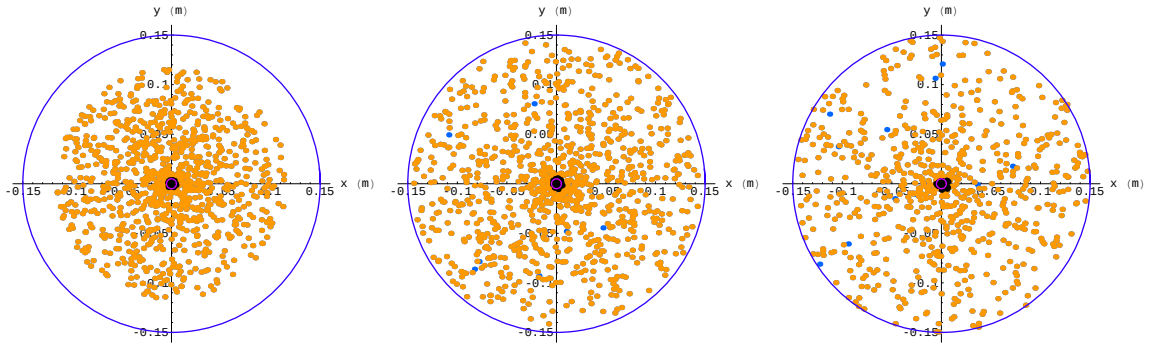

Figure 9: Simulation of an ideal muon track on the mirror. The left plot is for $L_f = 20\ cm$, the central plot is for $L_f = 25\ cm$, and the right plot is for $L_f = 35\ cm$.

of Cherenkov wavelengths between 350 and 450 nm. The plots are a view of the position of the photons as seen from above the mirror. The blue (small) dots show the location where the photons strike the mirror. The black (dark) dots are the location of the photons at the focal surface, L_f away from the center of the mirror. The black dots inside the small orange circle of radius 5 mm are considered detected. The orange dots correspond to the location of the "detected" photons on the mirror. We simulated 1000 photons for each of these plots. After scaling this to correspond to 200 photons per cm of useful track, we calculate that we should see 4000, 4960, and 4837 photons for $L_f = 20,\ 25,\ 35\ cm$, respectively. For the short focal length we consider only the light generated after the focal plane. Obviously, in all cases only the light that falls on the mirror is considered. This is evident in the figure for $L_f = 20cm$.

In Figure 10 we show the calculated photon intensity distribution for vertical muons rays that pass 3 cm away from the center of the mirror. The detected number of photons per muon is 239, 251, 223 for $L_f =\ 20,\ 25,\ 35\ cm$, respectively. It is instructive to see that the size of the image increases with the focal length, however the focal length cannot be reduced indefinitely for a given size mirror because we start losing useful length of muon track and thus the total amount of light on the mirror.

In Figure 11 we show the calculated photon intensity distribution for vertical muons rays that pass 3 cm away from the center at a height of 1 meter from the bottom on the mirror and have an angle of 1.7 deg, tilting in the positive y direction (so that they cross the upper right hand corner of the scintillator counter below the mirror). The detected number of photons per muon is 101, 32, 6 for $L_f =\ 20,\ 25,\ 35\ cm$, respectively. Angular divergence

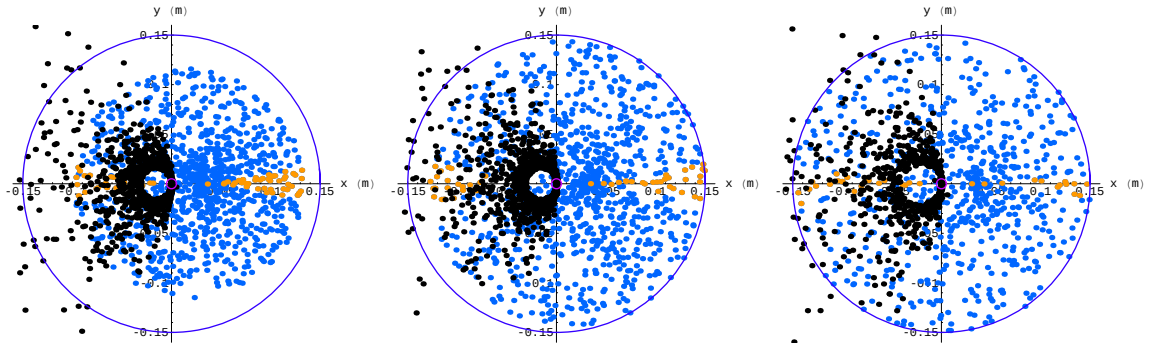

Figure 10: Simulation muon track 3 cm away from the center but vertically incident on the mirror. The left plot is for $L_f = 20\ cm$, the central plot is for $L_f = 25\ cm$, and the right plot is for $L_f = 35\ cm$.

of the muons moves the image on the focal plane causing blind spots in the center. It is possible to collect more photons in the "detector" if we place the detector deliberately away from the focal point. Such a strategy will increase the yield of photons from off-angle muons, but will reduce the yield from very vertical muons.

We have calculated the photon yields for the field of expected muon tracks, traversing two $6cm \times 6cm$ scitillation counters placed 1 meter apart. The distributions are shown in Figures 12, 13, and 14 for $L_f = 20,\ 25,\ 30\ cm$, respectively.

The histograms shows the distribution of the number of photons incident on a 1 cm diameter circle at the focal point as well as at $+10mm$ from the focal point. As can be seen any of the mirrors will produce pulses of good intensity with a rate of ~ 2 per hour. These photons will arrive at the detector with $< 0.2\ ns$ spread. Muons of angles $> 1.7^o$ produce zeros if the detector is placed at the focal point. The rate of zeros could be reduced significantly if we move the detector away from the focal point at the price of reducing pulse intensity for "bulls eye" muons. The rate of good muons can be increased by using several pairs of scintillation counters to widen the area over which muons are selected while keeping the angle of muons restricted to be vertical.

It should be remarked that for short focal lengths the photons are incident on the detector at a smaller glancing angle. This will cause higher reflection, and should be avoided. This consideration along with the distributions in the figures will determine the value of the focal length we will use.

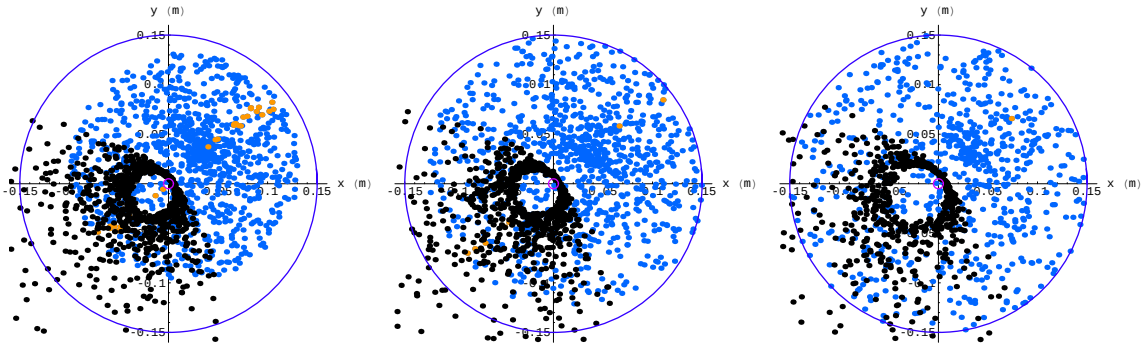

Figure 11: Simulation of muon tracks 3 cm away and at an angle of 1.7 deg as explained in the text. The left plot is for $L_f = 20\ cm$, the central plot is for $L_f = 25\ cm$, and the right plot is for $L_f = 35\ cm$.

The geometry explored in this note promises to be an interesting source of light for testing photo-sensors. We have not found any reason this technique should not work. Indeed, this geometry may have some interesting application in particle detection for fixed target accelerator experiments high energy physics. It allows very precise measurement of particles that have relatively small phase space. Using the numbers in this note a set of specifications for the mirror including precision ($< 5\mu m$) and alignment tolerance ($\sim 1mm$) can be made. We will get quotes from some manufacturers and also put together a tank as soon as possible.

References

[1] Review of particle physics, Physics Letter B, Vol. 592, (2004), Page 252.

[2] Handbook of Chemistry and Physics, David R. Lide (Editor-in-chief), 85th edition, CRC press, (2004-2005).

[3] R. M. Pope and E. S. Fry, "Absorption spectrum (380?700nm) of pure water. II. Integrating cavity measurements," Appl. Opt., 36, 8710–8723, (1997).

[4] R. C. Smith and K. S. Baker, "Optical properties of the clearest natural waters (200-800nm)," Appl. Opt., 20, 177–184, (1981).

[5] T. I. Quickenden and J. A. Irvin, "The ultraviolet absorption spectrum of liquid water," J. Chem Phys., 72, 4416–4428, (1980).

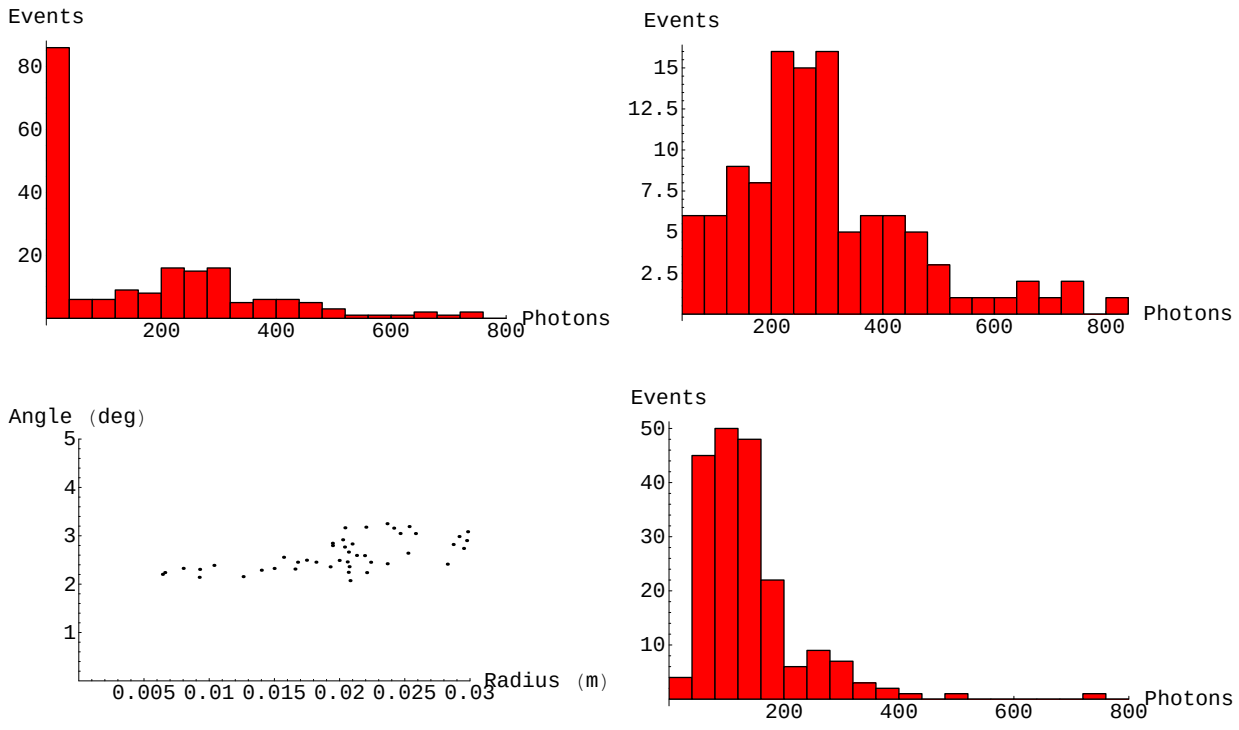

Figure 12: Distributions for a mirror with a focal length of 20 cm using 200 muons tracks defined by the scintillator counters as described in the text. Distribution of the number of photons incident on the detector (upper left). 56 Muons produced zero photons. Distribution of the number of photons without the first bin (upper right). Radial distance and the angle with respect to the vertical of muons that produced zero photons into the detector (lower left). The lower right is the distribution of incident photons with the detector placed 1.0 cm from the focal point.

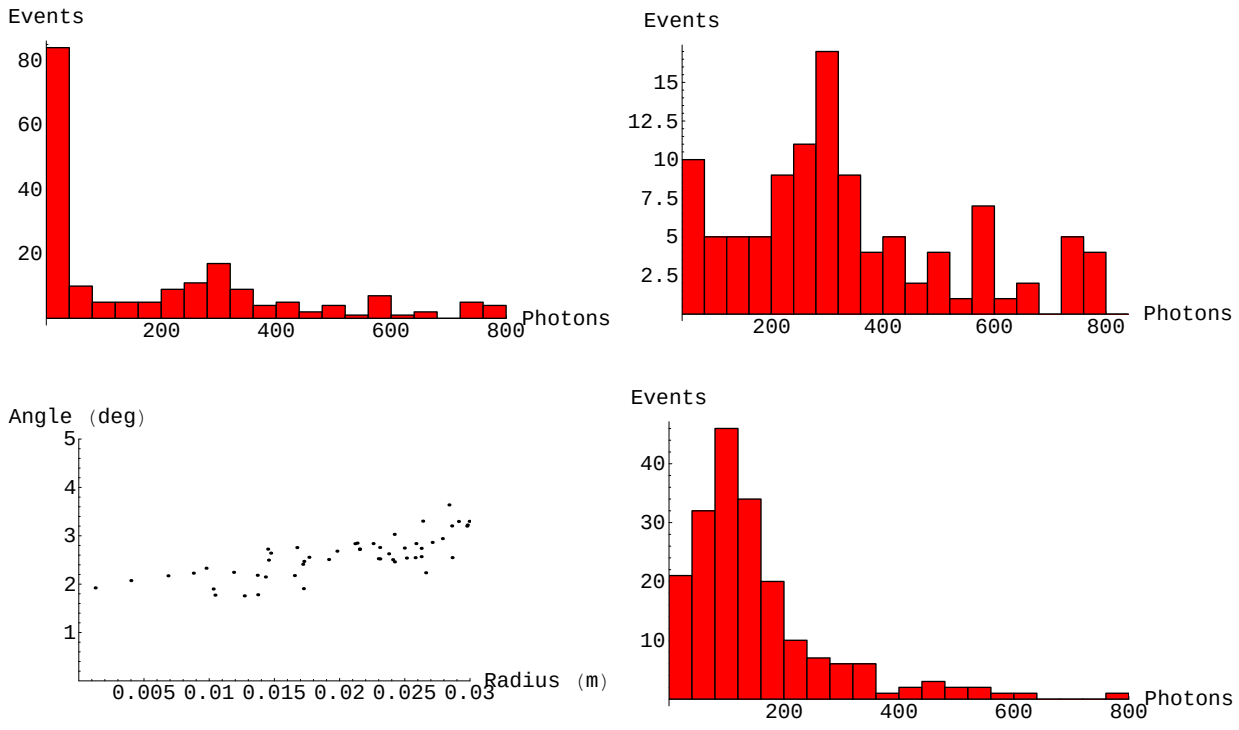

Figure 13: Distributions for a mirror with a focal length of 25 cm using 200 muons tracks defined by the scintillator counters as described in the text. Distribution of the number of photons incident on the detector (upper left). 62 muons had zero photons in this distribution. Distribution of the number of photons without the first bin (upper right). Radial distance and the angle with respect to the vertical of muons that produced zero photons into the detector (lower left). The lower right are the distribution of incident photons with the detector placed 1.0 cm from the focal point.

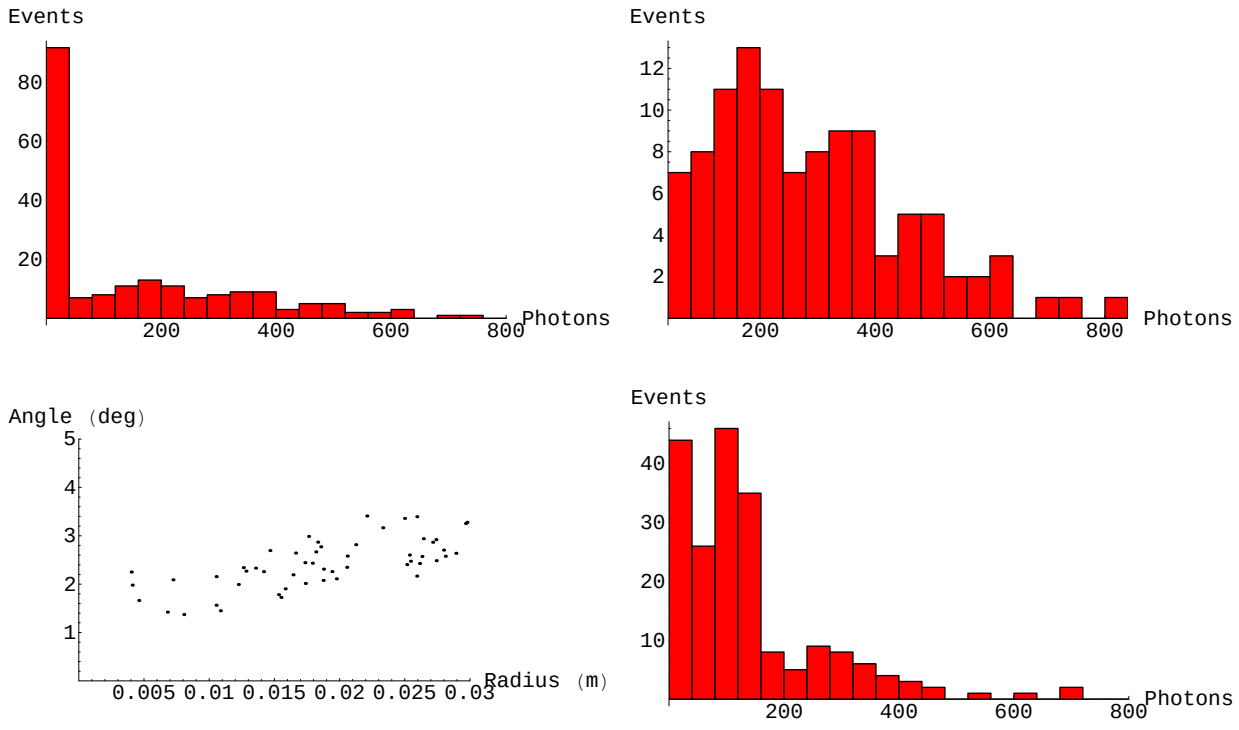

Figure 14: Distributions for a mirror with a focal length of 30 cm using 200 muons tracks defined by the scintillator counters as described in the text. Distribution of the number of photons incident on the detector (upper left). 62 muons had zero photons in this distribution. Distribution of the number of photons without the first bin (upper right). Radial distance and the angle with respect to the vertical of muons that produced zero photons into the detector (lower left). The lower right is the distribution of incident photons with the detector placed 1.0 cm from the focal point.

[6] A. C. Tam and C. K. N. Patel, "Optical absorption of light and heavy water by laser optoacoustic spectroscopy," Appl. Opt., 18, 3348–3358, (1979).

[7] S. Fukuda, et al., "The Super-Kamiokande Detector," Nuclear Instruments and Methods in Physics Research A501 (2003) 418-462.